# Double ionisation of disulfur

**Emelie Olsson[1], Tarek Ayari[2], Veronica Ideböhn[1], Måns Wallner[1], Richard J. Squibb[1], Mohamed Cheraki[2], Jonas Andersson[1], Andreas Hult Roos[1,3], John M. Dyke[4], John H.D. Eland[5], Majdi Hochlaf[2,*], and Raimund Feifel[1,*]**

[1]University of Gothenburg, Department of Physics, Origovägen 6B, 412 58 Gothenburg, Sweden
[2]Université Gustave Eiffel, COSYS/LISIS, 5 Bd Descartes 77454, Champs sur Marne, France.
[3]ELI Beamlines, Institute of Physics AS CR, v.v.i., Na Slovance 2, 182 21 Prague 8, Czech Republic
[4]School of Chemistry, University of Southampton, Highfield, Southampton SO17 1BJ, UK
[5]Oxford University, Department of Chemistry, Physical and Theoretical Chemistry Laboratory, South Parks Road, Oxford OX1 3QZ, United Kingdom
[*]majdi.hochlaf@univ-eiffel.fr, raimund.feifel@physics.gu.se

## ABSTRACT

Using time-of-flight multiple electron and ion coincidence techniques in combination with a helium gas discharge lamp and synchrotron radiation, the double ionisation spectrum of disulfur ($S_2$) and the subsequent fragmentation dynamics of its dication are investigated. The $S_2$ sample was produced by heating mercuric sulfide (HgS), whose vapour at a suitably chosen temperature consists primarily of two constituents: $S_2$ and atomic Hg. A multi-particle-coincidence technique is thus particularly useful for retrieving spectra of $S_2$ from ionisation of the mixed vapour. The results obtained are compared with detailed calculations of the electronic structure and potential energy curves of $S_2^{2+}$ which are also presented. These computations are done using configuration interaction methodology. The experimental findings are strongly supported by the theory.

## Introduction

Disulfur, $S_2$, is a reactive intermediate molecular species, which is of great interest from both a fundamental perspective, due to its similarity to molecular oxygen, and ~~also for a~~ number of applied scientific fields. In particular, it is astrophysically significant, and is especially important in the atmospheres of Jovian planets. Disulfur is a known constituent of the atmosphere of Io, from the plume above Mt. Pele[1]. Other charged sulfur ions are also known to exist in the torus around Europa[2] and in the ionosphere of Jupiter[3]. Furthermore, $S_2$ is a component of Comet IRAS–Araki–Alcock (1983 d)[4,5] and of the coma of comet 67P/Churyumov–Gerasimenko[6], but its origin in comets, for which several scenarios were proposed[7], is not known ~~yet~~. Disulfur also plays a significant role in magmatic and volcanic processes on earth[8]. ~~Apart from that, disulfide~~ bonds are very important in the stabilisation of protein structures[9].

The $S_2$ molecule has 12 valence electrons, which gives the following ground state electronic configuration, where the inner shell orbitals are omitted for simplicity:

$$\ldots 1\sigma_g^2 1\sigma_u^2 2\sigma_g^2 2\sigma_u^2 3\sigma_g^2 1\pi_u^4 1\pi_g^4 3\sigma_u^2 4\sigma_g^2 4\sigma_u^2 5\sigma_g^2 2\pi_u^4 2\pi_g^2.$$

As in molecular oxygen, the neutral ground state has $^3\Sigma_g^-$ symmetry, the first excited state is $^1\Delta_g$ and the second excited state is $^1\Sigma_g^+$. The ground state of the doubly charged ion comes from removal of the two outermost $\pi_g$ electrons and so is a $^1\Sigma_g^+$ state. The single ionisation electron spectrum of $S_2$ reported by Dyke and coworkers[10] was compared with spectra at 21.22 eV photon energy measured in the present work and used with other evidence ~~to~~ to verify the presence of $S_2$. Dyke et al.[10] found the lowest single ionisation energy to be 9.38 eV. According to the rule-of-thumb for double ionisation[11], $\mathrm{DIE} = (2.2 \pm 0.03)\mathrm{IE} + (11.5 \pm 1)/r_{12}$, and using an internuclear distance of 1.889 Å[12], we expect the lowest double ionisation energy of $S_2$ to be approximately 26.5 eV. In contrast, electron-impact experiments performed by Zavilopulo et al.[13] previously reported a surprisingly low value of 16.8 eV for the double ionisation of $S_2$.

In this paper, we present measurements of single-photon double ionisation electron spectra of $S_2$, thus characterising the electronic structure of $S_2^{2+}$ for the first time. The experimental spectra are obtained by irradiating the vapour produced from heated mercuric sulphide (HgS), whose main constituents at suitable temperatures are $S_2$ and atomic Hg[14]. For the experiments, we used both He II emission lines provided by a home-laboratory gas-discharge lamp and tuneable soft X-rays provided by ~~an~~ synchrotron radiation facility. Because atomic Hg gives very strong single and double ionisation signals and is highly abundant in these experiments, multi-particle coincidence experimental and analysis techniques are essential to select the double ionisation electron spectra of $S_2$.

~~For the~~ data interpretation~~, we computed the~~ potential energy curves of the lowest states of $S_2^{2+}$ using a multi-configuration

approach. We thus deduced the vertical ionisation energy of ~~$S_2^{2+}$~~, and determined a set of spectroscopic data for its (meta)stable states. Additionally, the potentials of $S_2$ and ~~of~~ $S_2^+$ were calculated, for validation and to deduce the adiabatic double ionisation energy of $S_2^{2+}$. Comparison of our detailed calculations of the electronic structure, potential energy curves and energetics of $S_2^{2+}$ with the experimental results confirms the formation of this dication upon doubly photoionising the vapour over heated HgS.

## Experimental details

The experiments were performed in our laboratory at the University of Gothenburg and the UE52_SGM beamline at the BESSY-II storage ring of the Helmholtz-Zentrum in Berlin, where our magnetic bottle electron spectrometer was augmented with an in-line ion time-of-flight spectrometer, similarly configured as presented previously in Refs.[15,16]. Utilising multi-coincidences of electrons and ions, it is possible to ~~filter on~~ specific ions when extracting electron pairs originating from double ionisation of $S_2$, thus rigorously eliminating contamination from Hg.

In the experimental set-up used, a hollow ring magnet with a hollow conical pole-piece, located about 10 mm away from the light matter interaction point, provides a divergent magnetic field which ~~directs the electrons into a~~ $\approx$ ~~2.2 m long flight tube~~. A solenoid surrounds ~~this~~ electron flight tube ~~and its~~ homogeneous field guides the electrons towards a micro-channel plate detector. The detector registers the flight time of the electrons, which are converted into energies based on an established calibration procedure which relies on known single ionisation and autoionisation energies described below. The electron kinetic energy ~~resolution~~ for this setup is E/$\Delta$E = 20 and the overall collection-detection efficiency is about 50 %[15]. A few hundred nanoseconds after photo~~absorption~~, once the electrons have escaped the interaction region, an electric field is applied across the interaction region in order to accelerate the ions through the ring magnet in the opposite direction to the electrons. ~~These~~ ions travel through a 0.12 m long flight tube towards a second micro-channel plate detector. The electric fields are optimised to obtain time focusing Wiley-McLaren conditions[17]. The flight time for the ions is proportional to $\sqrt{m/q}$, where $m/q$ is the mass to charge ratio. The mass resolution is $\approx$ 50 full-width-half-maximum (FWHM) and the collection-detection efficiency is about 10 %. ~~To reduce the~~ number of accidental coincidences, where ions and electrons from different ionisation events are detected together, the ionisation rate in the interaction region ~~is kept~~ below 2 %.

At the University of Gothenburg, a helium gas discharge lamp was used as a light source, providing few-nanosecond pulses of both He I and He II radiation of sufficiently high flux at a repetition rate of 4 kHz. The He II$\alpha$ atomic emission line at 40.81 eV was used for the double ionisation measurements. The synchrotron radiation experiments were performed ~~when the~~ BESSY-II storage ring ~~was operated~~ in single-bunch mode, at the photon energies of 90 eV and 180 eV. Single bunch operation is critical for this type of experiment, because it implies a time-separation of the radiation pulses of 800.5 ns, which, in turn, allows us to employ a mechanical chopper system to further reduce the pulse repetition rate[18] to $<$ 10 kHz as required by our multi-electron-ion coincidence technique.

In the light-matter interaction region of our spectrometer the radiation pulses intercept the effusive vapour produced by heating mercury(II) sulfide (Sigma Aldrich 243566-50G) in a resistively heated oven. The oven was operated at a temperature of 320 °C at the synchrotron radiation facility and at 280 °C in Gothenburg. The lower temperature proved preferable, since the vapour had similar composition to that produced at higher temperatures, but resulted in greater sample longevity.

In Gothenburg, the single ionisation electron spectra of molecular oxygen obtained at 21.22 and 40.81 eV were used for the time-of-flight to electron kinetic energy calibration, together with autoionisation energies for atomic Hg at 40.81 eV (see Ref.[19] and refs. therein). For the data sets at 90 and 180 eV from BESSY-II, the double ionisation and autoionisation energies of Hg were used as internal calibrants.

## Computational details

The potential energy curves of the electronic states of $S_2^{2+}$ in the singlet, triplet, quintet and septet spin multiplicities were computed using highly correlated *ab initio* methods, such as the state-averaged complete active space self-consistent field (SA-CASSCF) approach[20,21] followed by the Multi-Reference Configuration Interaction (MRCI) method[22–24] as implemented in MOLPRO 2015[25,26]. For the description of the sulfur atom, we used the aug-cc-pV(5+d)Z basis set[27–29]. The inclusion of the tight-d functions is necessary for a good description of the sulfur atoms. From this, the energetic profiles for the dissociation of the molecule can be produced, including both the $S^+$ fragments in their ground states ($^4S_u$) and/or where one of the two asymptotes for the sulfur ions are in an excited state ($^2D_u$ and/or $^4S_g$). Also, using the restricted coupled cluster single-double(-triple) (RCCSD(T)) level of theory[30–32] with the same basis set, the double ionisation energy of $S_2$ and the lowest dissociation limits of $S_2^{2+}$ have been determined. The basis set superposition error (BSSE) correction has been included, but amounted to only 0.01 eV. For the states having a potential well, their potential energy curves was incorporated into nuclear motion treatment to deduce their rotational and vibrational spectroscopic constants using the method of Cooley[33] and the derivatives at the minimum energy distances and standard perturbation theory. For validation of the present approach, we computed the potential energy curves of $S_2$ and of $S_2^+$ in their electronic ground states. The results are given in Table 1, together

with their comparison with the available experimental data. As can be seen there is a good agreement with the experimental results. Also, we compute an adiabatic ionisation energy of $S_2$ of about 9.26 eV which is close to the experimental value of 9.38 eV[10]. Therefore, the computed data for $S_2^{2+}$ dication should be of similar accuracy.

**Table 1.** Spectroscopic constants of the ground electronic states of $S_2$ ($X^3\Sigma_g^-$) and $S_2^+$ ($X^2\Pi_g$).

| State | | $R_e$ (Bohr) | $\omega_e$ ($cm^{-1}$) | $\omega_e x_e$ ($cm^{-1}$) | $\omega_e y_e$ ($cm^{-1}$) | $B_e$ ($cm^{-1}$) | $\alpha_e$ ($cm^{-1}$) |
|---|---|---|---|---|---|---|---|
| $S_2$ ($X^3\Sigma_g^-$) | Calc. | 3.5881 | 719.8 | 2.8 | 0.00271 | 0.29224 | 0.00158 |
| | Exp.[34–37] | 3.5701 | 725.65 | 2.844 | | 0.2954 | 0.001570 |
| $S_2^+$ ($X^2\Pi_g$) | Calc. | 3.4630 | 799.6 | 3.4 | 0.00432 | 0.31374 | 0.00171 |
| | Exp.[38] | 3.4467 | 806.099 | 3.3971 | | 0.316974 | |

## Results and Discussion

Fig. 1 shows three variants of the mass spectrum of mercury sulfide vapour obtained at a photon energy of 40.81 eV. The lower spectrum (dashed blue line) includes all ions produced at this energy and is dominated by single and double ionisation signals of Hg as well as $S_2^+$ and $S^+/S_2^{2+}$. The middle (solid orange line) spectrum shows an intensified version of the spectrum magnified by a factor of 10 and the intensities of the strongest peaks truncated so as to emphasise the weaker features. Here, we can also identify several sulfur oligomers, up to $S_8^+$. Inspection of the single ionisation electron spectrum shows that $S_2$ is produced mainly in its $^3\Sigma_g^-$ ground state[10], but a small proportion of excited molecules in the $^1\Delta_g$ state, about 0.5 eV higher in energy[39] cannot be ruled out. The upper (solid red line) spectrum in Fig. 1 shows ions extracted in coincidence with two electrons, where the singly charged species must originate from charge-separation processes of nascent doubly charged molecular species.

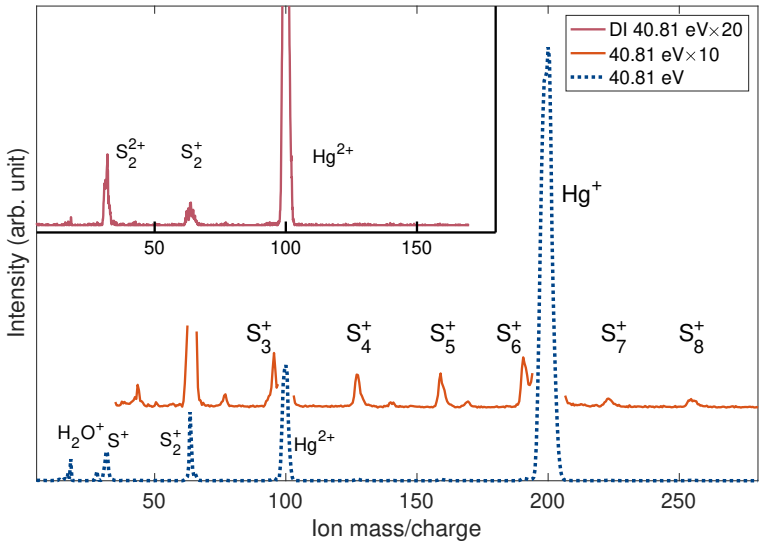


**Figure 1.** Full mass spectrum of the vapour of heated HgS at 40.81 eV (dashed blue line), with x10 magnification (solid orange line), and the spectrum of ions extracted in coincidence with two electrons (solid red line). The spectra are dominated by Hg, followed by $S_2$.

Fig. 2 shows similar spectra obtained using synchrotron radiation. The lower (dashed grey line) mass spectrum shows all single ions in coincidence with single electrons with binding energy in the range 5-20 eV, obtained at a photon energy of 90 eV, which is again dominated by ionisation of Hg. The x10 enlargement (solid green line) reflects several sulfur species. We note that the $S^+$ feature also contains $S_2^{2+}$, and from its width and shape seems to be dominated by fragmentation of $S_2^{2+}$. The upper (solid purple line) spectrum was obtained at 180 eV and contains both Hg and sulfur species, in particular a strong signal of $S^+$ / $S_2^{2+}$. In this case, the ions were filtered by selection of the majority of double ionisation events from Auger decay of an initial S 2p hole, selected on the photoelectron kinetic energy ~~of~~ 6-12 eV. At this photon energy a minority of electrons also comes

from valence double ionisation[19,40], and from multiple Auger decays producing triple and quadruple ionisation, explaining the presence of multiply charged ions in the spectrum. At slightly higher photon energy (not shown) core-valence ionisation[41] can also contribute.

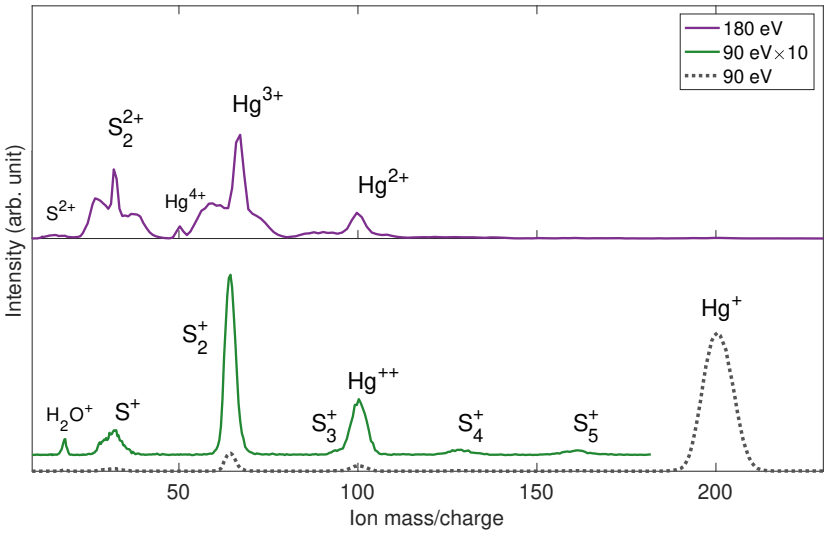


**Figure 2.** Lower panel: Mass spectra reflecting primarily singly charged ions, which were extracted in coincidence with one electron of a binding energy ~~of~~ 5-20 eV, obtained at a photon energy of 90 eV (dashed grey line and solid green line). The spectrum in grey is dominated by $Hg^+$. The orange plot is x10 magnification of that part of the spectrum which is relevant for the discussion. The full-width-half-maximum of the $S^+$ signal suggests substantial contributions from fragmentation of $S_2^{2+}$. Upper panel: a mass spectrum reflecting ions detected in coincidence with two electrons, obtained at a photon energy of 180 eV (solid purple line). At this photon energy the double ionisation route by Auger decay of the S 2p core holes is dominant.

Since the species $S_2^{2+}$ and $S^+$ have the same mass to charge ratio (m/q = 32), their features coincide in the mass spectra. $S^+$ originating from dissociation of the dimer dication, $S_2^{2+} \rightarrow S^+ + S^+$, will have a kinetic energy release, which will lead to a broadening of the spectral feature. This broadening is very substantial in the 180 eV ~~data,~~ leading to the formation of distinguishable, separated 'wings'. However, the sharper centre of the peak at m/q = 32, which corresponds to ions with little to no initial kinetic energy, could also be contaminated by contributions from nascent atomic $S^+$ produced directly by the source. Hence, the peak at m/q = 32 in the unfiltered spectrum (dashed grey line) may contain contributions from atomic $S^+$, the fragmentation of $S_2^{2+}$, and possibly $S^+$ from fragmentation of more highly charged $S_2$ ions or higher mass sulfur oligimers.

To determine how much atomic S might be present in the vapour, the relative intensity of the peak at m/q = 32 can be compared to $Hg^{2+}$ in Fig. 1. The intensity difference for the $Hg^{2+}$ peak between the blue and the red spectra could, in principle, be affected by possible differences in accidental coincidences, but is more likely to be affected by the collection-detection efficiencies when selecting one extra electron. By comparing to $Hg^{2+}$, the conclusion is that at least half the intensity in the m/q = 32 peak in the full spectrum must be associated with dissociation of $S_2^{2+}$.

According to previous studies of HgS vapour, the fraction of atomic S increases with sample temperature[14], and we would therefore expect to see a greater fraction of atomic S in the vapour for the higher temperature (320 °C) data sets compared to the lower temperature (280 °C) data sets. The higher temperature data sets were obtained at 90 and 180 eV, whose mass spectra are shown in Fig. 2. Here, the grey and green spectra comprise events involving one ion and one electron, and therefore includes contributions from all single ionisation processes. Double ionisation can also be seen in these spectra if only one of the emitted electrons is detected, why we see doubly charged Hg. The peak at m/q = 32 in these spectra could then be expected to include contributions from ionised atomic S, $S_2^{2+}$ or $S^+$ from oligimer dissociation. However, the broad width of the peak and lack of a sharp, central feature suggests little contribution from low kinetic energy ions, and instead comes predominantly from molecular dissociation, implying that there is hardly any atomic S present in the mass spectra.

Conversely, spectra where only ions detected in coincidence with two electrons were extracted (e.g. the purple spectrum taken at 180 eV), there should be hardly any contribution from nascent S since the emission of two electrons from this species would result in a $S^{2+}$ final state (m/q = 16). In these cases, ions of m/q = 32 must come almost exclusively from charge-retaining dissociation events of molecular sulfur species. The exception would be in the case that there are significant

differences in the accidental coincidences, however we expect this to be unlikely given our aforementioned coincidence conditions. We can therefore ensure the removal of any contributions from nascent S by restricting our dataset to two-electron processes that are coincident with an ion at m/q 32.

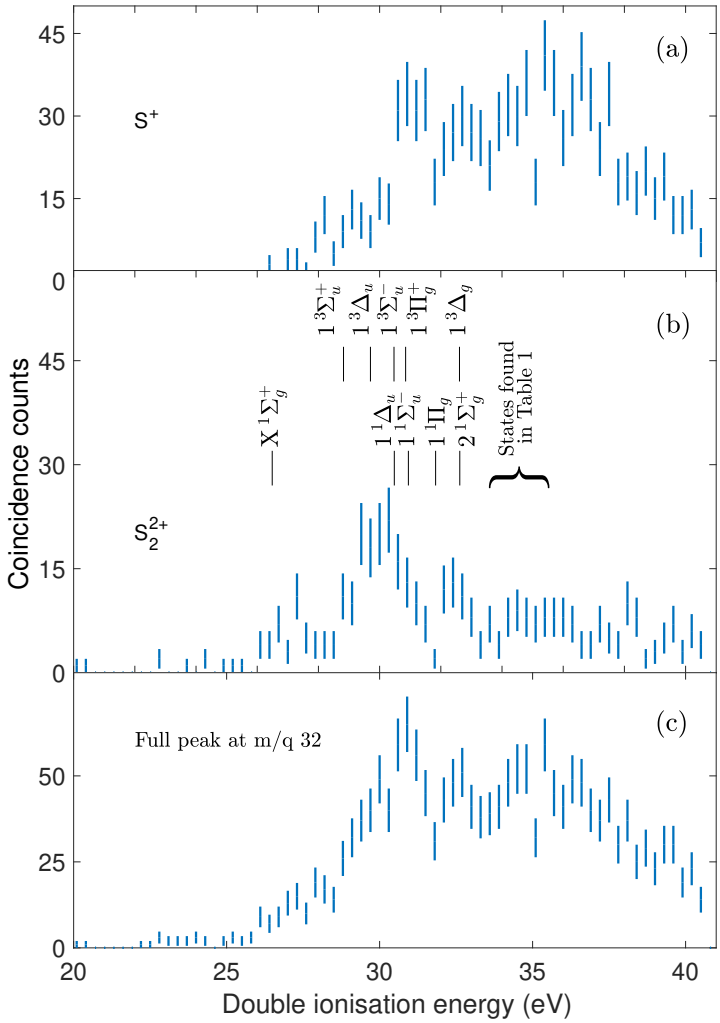


**Figure 3.** Double ionisation electron spectra from electron-ion coincidences at the photon energy of 40.81 eV. Each spectrum is based on electron pairs extracted in coincidence with all ions at mass/charge of 32 (c), $S_2^{2+}$ ion (b) or one of its $S^+$ fragments (a). The middle panel also shows calculated vertical excitation energies from the ground state of neutral $S_2$. All states can be found in Table 2.

The double ionisation spectra of the $S_2^{2+}$ and the $S^+ + S^+$ species can be obtained by selecting the two electrons in coincidence with the corresponding ion, and then subtracting the kinetic energy sum of the two electrons from the known photon energy. These spectra are shown in Fig. 3(a) for $S^+$ and (b) for $S_2^{2+}$ for a photon energy of 40.81 eV. The bottom (c) panel shows the complete double ionisation spectrum, where the two electrons were correlated with the entire ion peak centred around at m/q = 32. For the (b) and (a) panels, electron pairs associated primarily with $S_2^{2+}$ or $S^+$ have been extracted, by selecting the narrow part of the peak and the higher kinetic energy wings, respectively. We also expect some contribution from $S^+$ in the narrow part of the peak, but subtraction of spectrum 3(a) from 3(b) shows no appreciable difference.

From the $S_2^{2+}$ spectrum seen in Fig. 3(b), it is apparent that the lowest double ionisation energy is located around 27 eV where a first, comparatively sharp feature is observed, while the most intense peak is observed very near 30 eV. The maximum of the first peak corresponds to the vertical double ionisation energy of $S_2$, and the non zero signal starting slightly above 26 eV may correspond to the adiabatic double ionisation energy of $S_2$. Both values are expected to differ since non favorable Franck-Condon factors upon double ionising $S_2$ are expected (see explanation below). Based on the FWHM of the $Hg^{2+}$ $X^1S_0$ state, the estimated electron resolution at 40.81 eV is 0.8 eV.

For the $S^+$ spectrum shown in Fig. 3(a), the appearance energy is somewhat higher, nearer to 30 eV, with the first strong feature at about 31 eV. The thermodynamic threshold for $S^+ + S^+$ from $S_2$ is 25.14 eV, which implies an excess energy of 5 eV, which could be mainly kinetic energy, possibly with some excitation of the atomic sulfur ions. A kinetic energy release of this magnitude is confirmed by calculations based on the width of the m/q = 32 ion peak in the time of flight spectra and simulations of the electric field in the interaction region.

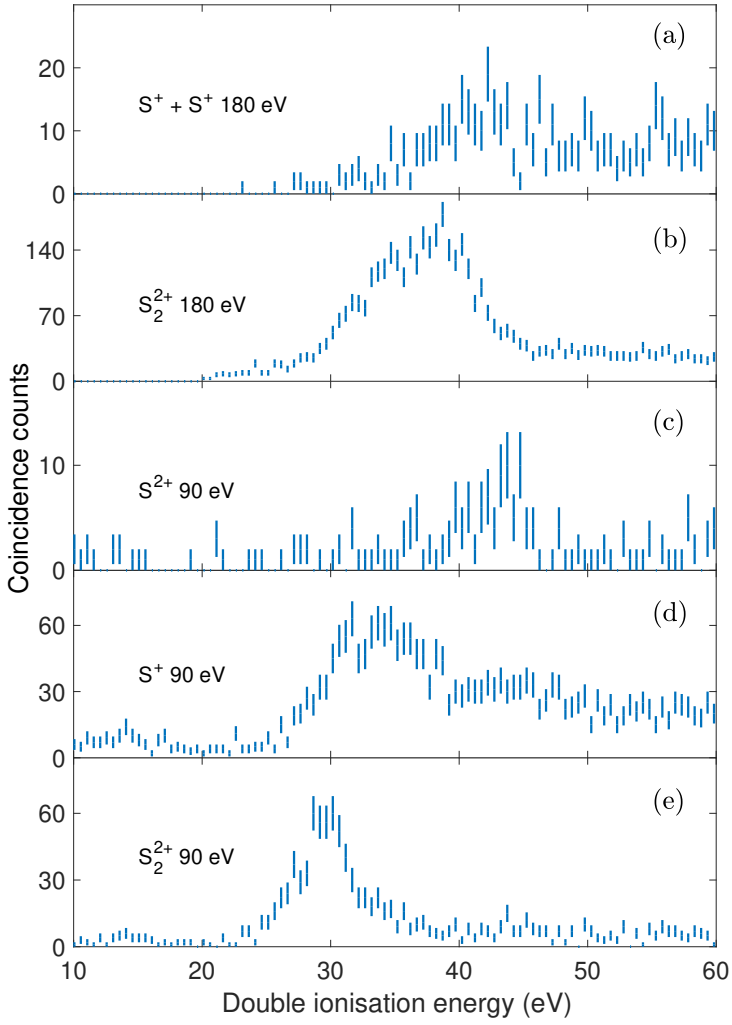


**Figure 4.** Double ionisation electron spectra obtained at the photon energies of 90 and 180 eV, based on electron pairs in coincidence with $S_2^{2+}$, $S^+$ or $S^{2+}$ signals.

For comparison, Fig. 4 shows the double ionisation spectra of the vapour of mercuric sulfide obtained at the photon energies of 90 eV and 180 eV, respectively. The spectra show electron pairs selected in coincidence with ions, either on the narrow central peak of the m/q = 32 feature in Fig. 2, primarily representing $S_2^{2+}$ species, or the wings around m/q = 32 primarily associated with $S^+$ species. The relative intensities of the different spectra are to be taken with caution, since some of the high kinetic $S^+$ may had high enough off-axis velocity components to hit sufaces and so evade detection. Also, the shapes of the features at the two photon energies are not expected to be the same, partly because energy resolution is better at the lower photon energy, but more importantly because the ionisation processes are distinct in each case. At 90 eV, ionisation can be expected to be entirely from the valence shell, whereas at 180 eV double ionisation via Auger decay of a S 2p hole is dominant. The estimated electron resolution, based on the FWHM of the $Hg^{2+}$ $X^1S_0$ state, is 3 eV at 90 eV and 6 eV at 180 eV. From the $S_2^{2+}$ spectrum at 90 eV, a weak feature can again be discerned at 27.1 eV, whereas a stronger peak is observed around 30 eV. Electron pairs extracted in coincidence with $S^+$ again show a shift of the onset towards higher ionisation energies, akin to the 40.81 eV measurements described above. Also, in the 90 eV electron pair spectrum selected on m/q = 16 which corresponds to the $S^{2+}$ species, the signal starts around 40 eV. The formation of $S^{2+}$ can be expected to originate from charge-retaining

fragmentation of $S_2^{2+}$. Such charge retaining fragmentation could occur from more highly excited states, which is line with its onset around 40 eV.

For data obtained at the photon energy of 180 eV, the double ionisation electron spectra extracted in coincidence with $S_2^{2+}$ and $S^+$ can be seen in Fig. 4 (b) and (a) respectively. For Fig. 4(a), the spectrum is based on fourfold coincidences, with two $S^+$ ions and two electrons. The degradation in resolution at these comparatively high electron kinetic energies does not allow any sharp peaks to be identified, but the overall appearance of the spectra matches that of the 90 eV data. For the $S^+ + S^+$ channel, the high double ionisation energy explains the very high kinetic energy release we see in the mass spectrum (cf. Fig. 2, upper panel).

**Table 2.** Spectroscopic parameters and vertical double ionisation energies (VDIE) of $S_2^{2+}$ states, numbered in order of increasing VDIE.

| | State | $R_e$ (Bohr) | $\omega_e$ ($cm^{-1}$) | $\omega_e x_e$ ($cm^{-1}$) | $\omega_e y_e$ ($cm^{-1}$) | $B_e$ ($cm^{-1}$) | $\alpha_e$ ($cm^{-1}$) | VDIE (eV) |
|---|---|---|---|---|---|---|---|---|
| 0 | $X\,^1\Sigma_g^+$ | 3.372 | 832.2 | 1.07 | 0.67 | 0.33081 | 0.00199 | 26.49 |
| 1 | $1\,^3\Sigma_u^+$ | 3.853 | - | - | - | 0.25578 | 0.00894 | 28.82 |
| 2 | $1\,^3\Delta_u$ | 3.784 | 568.0 | 3.58 | 0.06 | 0.26271 | 0.00205 | 29.7 |
| 3 | $1\,^3\Sigma_u^-$ | 3.752 | 598.1 | 3.63 | 0.08 | 0.26730 | 0.00178 | 30.47 |
| 4 | $1\,^1\Delta_u$ | 3.747 | 612.3 | 5.41 | 0.25 | 0.26795 | 0.00176 | 30.48 |
| 5 | $1\,^3\Pi_g$ | 3.577 | - | - | - | 0.54900 | 0.5856 | 30.85 |
| 6 | $1\,^1\Sigma_u^-$ | | | | | | | 30.94 |
| 7 | $1\,^1\Pi_g$ | 3.632 | 588.4 | 2.02 | 0.32 | 0.28517 | 0.00260 | 31.83 |
| 8 | $1\,^3\Delta_g$ | | | | | | | 32.61 |
| 9 | $2\,^1\Sigma_g^+$ | 4.250 | 479.4 | 2.35 | 0.05 | 0.20831 | 0.00110 | 32.62 |
| 10 | $1\,^1\Sigma_u^+$ | 4.098 | 275.9 | - | - | 0.22415 | 0.00118 | 33.56 |
| 11 | $1\,^3\Pi_u$ | | | | | | | 33.8 |
| 12 | $1\,^1\Gamma_u$ | | | | | | | 33.86 |
| 13 | $1\,^1\Pi_u$ | | | | | | | 34.22 |
| 14 | $2\,^3\Pi_u$ | | | | | | | 34.41 |
| 15 | $1\,^3\Phi_u$ | | | | | | | 34.58 |
| 16 | $2\,^3\Pi_g$ | | | | | | | 34.86 |
| 17 | $1\,^1\Delta_g$ | | | | | | | 35.19 |
| 18 | $1\,^3\Sigma_g^+$ | | | | | | | 35.24 |
| 19 | $2\,^3\Sigma_u^+$ | | | | | | | 35.27 |
| 20 | $1\,^1\Phi_u$ | | | | | | | 35.28 |
| 21 | $2\,^3\Delta_g$ | | | | | | | 35.49 |
| 22 | $3\,^3\Pi_u$ | | | | | | | 35.56 |

For the interpretation of the experimental results, we make use of our *ab initio* computations on the potential energy curve of the neutral $S_2$ ($X^3\Sigma_g^-$) ground state and the potential energy curves of the lowest electronic states of $S_2^{2+}$ dication. The theoretical results are presented in Tables 2 and 3 and as potential energy curves for the gerade and ungerade states in Figs. 5 and 6, respectively. For the dication, the potential energy curves result in bound electronic states for lower double ionisation energies, whereas higher double ionisation energies efficiently lead to dissociation. In particular, a relatively deep potential well is computed for the ground electronic state of $S_2^{2+}$ confirming the long lived nature of this dication and observation of a peak in the mass spectra associated with $S_2^{2+}$. The formation of $S_2^{2+}$ ($X^1\Sigma_g^+$) is associated with the removal of two electrons from the outermost $2\pi_g^2$ molecular orbital, which is antibonding in nature. This results in a shortening of the S-S distance. For

instance, we calculated a S-S distance of 3.588 Bohr (= 1.898 Å) for $S_2$ ($X^3\Sigma_g^-$) and of 3.372 Bohr (= 1.784 Å) for $S_2^{2+}$ ($X^1\Sigma_g^+$) (cf. Table 1). Therefore, non favorable Franck-Condon factors are expected for the $S_2$ ($X^3\Sigma_g^-$) $\rightarrow$ $S_2^{2+}$ ($X^1\Sigma_g^+$) + 2 $e^-$ transition. In particular, the adiabatic double ionisation energy of $S_2$ should be difficult to deduce from the experimental spectra due to the lack of vibrationally resolved structures in contrast to the threshold photoelectron coincidence spectrum and the complete valence double ionisation electron spectrum of $O_2$[42,43].

**Table 3.** Dissociation limits for $S_2^{2+}$ leading to two $S^+$ fragments in their ground and excited states. The lowest asymptote is located experimentally as 25.14 eV above the vibrational ground state of neutral $S_2$[39,44]. The adiabatic double ionisation energy of $S_2$ is calculated as 26.31 eV, lying 1.18 eV above the lowest asymptote.

| Dissociation Fragments | Relative energy (eV) | Molecular States |
|---|---|---|
| $S^+(^4S_u) + S^+(^4S_u)$ | 0.00 | $^1\Sigma_g^+, ^3\Sigma_u^+, ^5\Sigma_g^+, ^7\Sigma_u^+$ |
| $S^+(^4S_u) + S^+(^2D_u)$ | 1.84 | $^{3,5}(\Sigma^+,\Pi,\Delta)_{u,g}$ |
| $S^+(^4S_u) + S^+(^2P_u)$ | 3.05 | $^{3,5}(\Sigma^-,\Pi)_{u,g}$ |
| $S^+(^2D_u) + S^+(^2D_u)$ | 3.68 | $^1(\Sigma_g^+(3),\Sigma_u^-(2),\Pi_g(2),\Pi_u(2),\Delta_g(2),\Delta_u,\Phi_g,\Phi_u,\Gamma_g)$, $^3(\Sigma_u^+(3),\Sigma_g^-(2),\Pi_g(2),\Pi_g(2),\Delta_g,\Delta_u(2),\Phi_g,\Phi_u,\Gamma_u)$ |
| $S^+(^2D_u) + S^+(^2P_u)$ | 4.88 | $^{1,3}(\Sigma^+,\Sigma^-(2),\Pi(3),\Delta(2),\Phi)_{u,g}$ |
| $S^+(^2P_u) + S^+(^2P_u)$ | 6.08 | $^1(\Sigma_g^+(2),\Sigma_u^-,\Pi_g,\Pi_u,\Delta_g)$, $^3(\Sigma_u^+(2),\Sigma_g^-,\Pi_g,\Pi_u,\Delta_u)$ |

The empirical rule-of-thumb for estimating double ionisation energies presented by Molloy et. al[11], $\mathrm{DIE} = (2.2 \pm 0.03)\mathrm{IE} + (11.5 \pm 1)/r_{12}$, with the values of 9.38 eV for the lowest single ionisation of $S_2$[10] and the bond distance of 1.889 Å for neutral $S_2$[12], ~~also~~ agrees with our double ionisation energy of 27 eV. Besides, our calculations predict the adiabatic double ionisation energy for $S_2$ to be 26.31 eV and the vertical double ionisation energy to be at 26.49 eV. Experimentally, we observe a weak feature at 27.1±3 eV (cf. Fig. 4(e)) for the $S_2^{2+}$ species at 90 eV, while the first signal of the $S_2$ double ionisation at 41 eV can be seen at 27±0.1 eV (cf. Fig. 3(b)). This feature is not discernible at the photon energy of 180 eV, most likely because of the lower resolution for electrons with higher kinetic energies. The present calculations allow assign~~ing~~ this band in the double ionisation spectrum to the population of $S_2^{2+}$ ground state.

The equilibrium bond distance in neutral $S_2$ is 3.588 Bohr (= 1.898 Å), so according to the calculated potential energy curves, vertical double ionisation can populate the first excited state at about 29 eV ($1^3\Sigma_u^+$), which also correlates directly to ground state products and so could explain the shoulder of the larger peak in Fig. 3(b). The next excited state is $1^3\Delta_u$ at about 30 eV, which might contribute to the feature we see for $S_2^{2+}$ in both Fig. 4(e) at 29.4±3 eV and Fig. 3(b) at 30±0.8 eV. The $1^3\Delta_u$ state has an equilibrium bond length close to the bond length of neutral $S_2$, and could produce a narrow peak. But as this state does not correlate to ground state products, it would have to be predissociated by a crossing quintet or septet state, and so ions in this state may persist as undissociated $S_2^{2+}$.

Our calculations also predict a $1^3\Pi_g$ state near 31.5 eV with ~~a~~ bond length similar to that of neutral $S_2$. This state appears mainly in the $S^+ + S^+$ channel, in both the 40.81 eV (see Fig. 3(a)) and 90 eV (see Fig. 4(d)) spectra. In comparison to $O_2$ double photoionisation, whose most prominent sharp feature is an analogous $^3\Pi_g$ state, we consider it likely to be responsible for the main peak seen near 31 eV in the spectra (see Fig. 3(a))[45,46]. Another similarity between the $S_2$ and $O_2$ double ionisation spectra is the distinct separation between the ground state $^1\Sigma_g^+$ and the first excited states[45].

Fig. 3(a) suggests that the $S_2^{2+}$ ion is stable to about 30 eV, which is also supported by the potential energy curves from the calculations. The threshold for decomposition into $S^+ + S^+$ seems to be about 30.5 eV, which lies between the $1^1\Delta_u$ and the $1^3\Pi_g$ state.

According to the potential energy curves (cf. Figs. 5 and 6), the $^1\Sigma_g^+$ ground state for the $S_2^{2+}$ correlates directly to ground state products. It is separated towards the $S^+ + S^+$ fragments by a potential barrier of about 3 eV. This leads to a computed appearance energy of 29.3 eV and a kinetic energy release of 4.3 eV. Both values are smaller by 0.7 eV compared to those deduced from the here presented double ionisation spectra of $S_2$. Besides, we may populate the electronic excited states of the dication lying at 30 eV (for a detailed assignment, cf. Fig. 3(b)). At least the $S_2^{2+}$ ($1^3\Delta_u$) state can be predissociated by the ($1^7\Sigma_u^+$) state involving spin-orbit interaction at their crossing (i.e. for energies of $\sim$ 4.5 eV above $S_2^{2+}$ ($X^1\Sigma_g^+$)). The septet correlates adiabatically to the lowest dissociation limit. We deduce an appearance energy of $\sim$ 30.8 eV and a kinetic energy release of $\sim$ 4.8 eV in close agreement with the measured values.

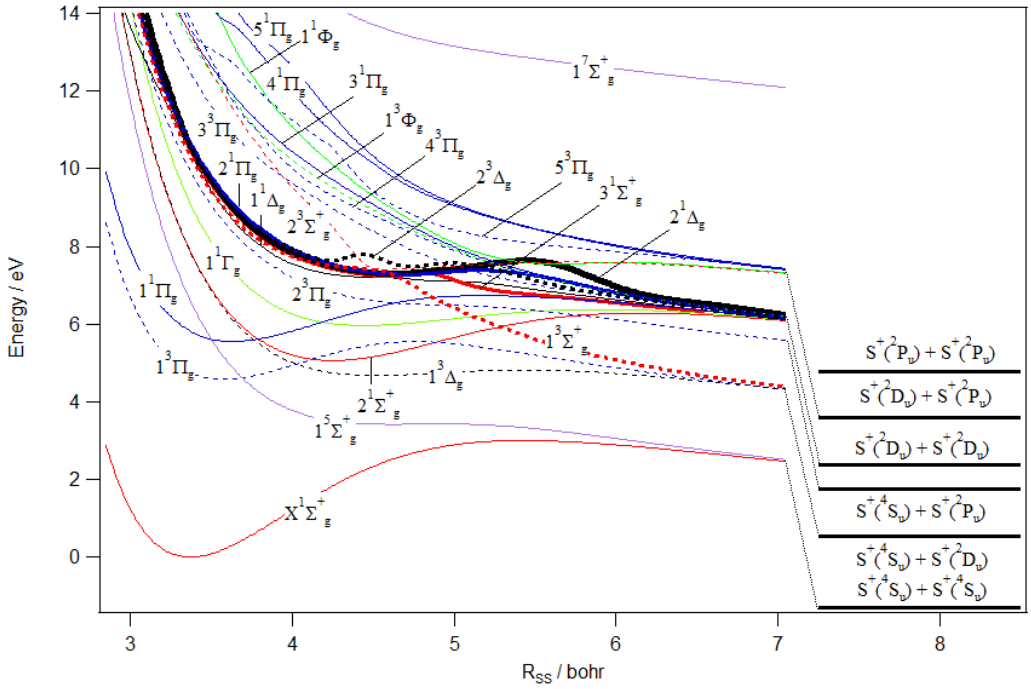


**Figure 5.** MRCI/aug-cc-pV(5+d)Z potential energy curves of $S_2^{2+}$. The reference energy is the energy of $S_2^{2+}(X^1\Sigma_g^+)$ at the equilibrium bond distance.

## Conclusions

We have presented a combined experimental and theoretical work on the double ionisation of disulfur. One of the main objectives of this study was to measure the first double ionisation electron spectrum of disulfur, $S_2$, and to determine the lowest double ionisation energy of this reactive intermediate. The double ionisation electron spectrum of $S_2$ showed many similarities with that of $O_2$, but with different energy separation between the states. The experimental results obtained from our electron-ion coincidence measurements at 40.81 eV and 90 eV showed very similar spectral structures for the two photon energies, revealing a vertical double ionisation energy of 27±0.8 eV. This lowest double ionisation energy is strongly supported by the empirical rule-of-thumb for double ionisation and by *ab initio* calculations. Also, a weakly excited first excited state at 28.8±0.8 eV was identified as $1^3\Sigma_u^+$ and a stronger peak near 30 eV as $1^3\Delta_u$. For the charge separated decay, the most prominent feature at 31.3±0.8 eV was identified as a $1^3\Pi_g$ state.

## Acknowledgements

This work has been financially supported by the Swedish Research Council (VR) and the Knut and Alice Wallenberg Foundation, Sweden. We thank the Helmholtz Zentrum Berlin for the allocation of synchrotron radiation beam time and the staff of BESSY-II for smooth operation of the storage ring in single-bunch mode. The research leading to these results has received funding from the European Union's Horizon 2020 research and innovation programme under grant agreement No 730872.

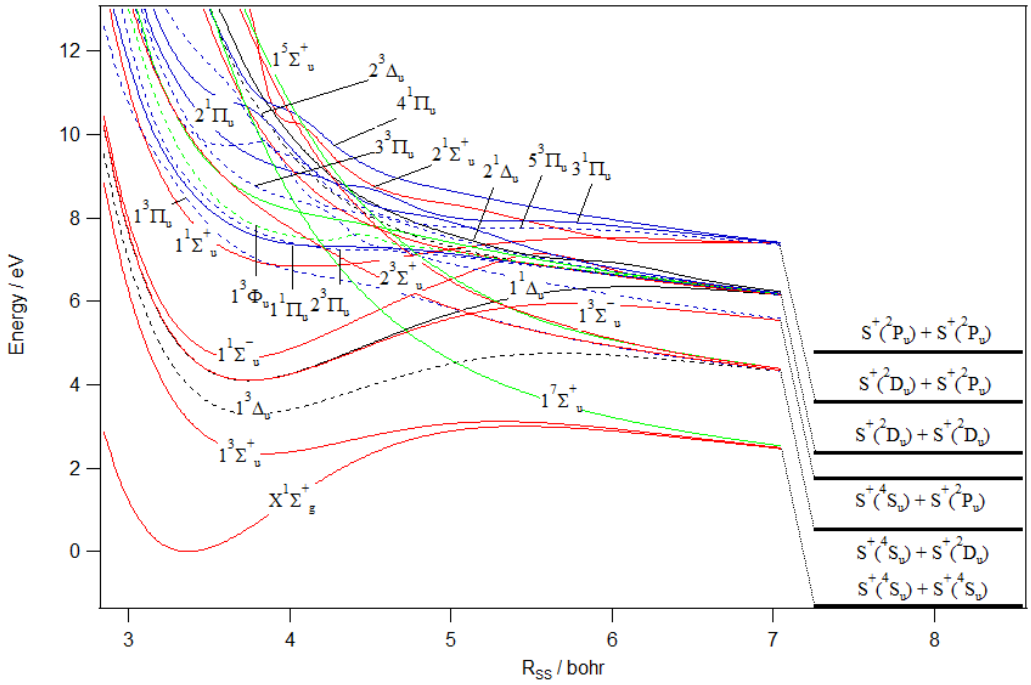


**Figure 6.** MRCI/aug-cc-pV(5+d)Z potential energy curves of $S_2^{2+}$. The reference energy is the energy of $S_2^{2+}(X^1\Sigma_g^+)$ at the equilibrium bond distance.

## References


1. Spencer, J., Jessup, K., McGrath, M., Ballester, G. & Yelle, R. Discovery of gaseous S2 in Io's Pele plume. *Science* **288(5469)**, 1208–1210, DOI: 10.1126/science.288.5469.1208 (2000).
2. Nénon, Q. & André, N. Evidence of europa neutral gas torii from energetic sulfur ion measurements. *Geophys. Res. Lett.* **46**, 3599–3606, DOI: 10.1029/2019GL082200 (2019).
3. Valek, P. W. *et al.* Jovian high-latitude ionospheric ions: Juno in situ observations. *Geophys. Res. Lett.* **46**, 8663–8670, DOI: 10.1029/2019GL084146 (2019).
4. A'Hearn, M. F., Schleicher, D. G. & Feldman, P. D. The discovery of S2 in comet IRAS-Araki-Alcock 1983d. *Astrophys. J.* **274**, L99–L103, DOI: 10.1086/184158 (1983).
5. Cosmovici, C. B. & Ortolani, S. Detection of new molecules in the visible spectrum of Comet IRAS-Araki-Alcock (1983 d). *Nature* **310**, 122–124, DOI: 10.1038/310122a0 (1984).
6. Calmonte, U. *et al.* Sulphur-bearing species in the coma of comet 67P/Churyumov-Gerasimenko. *Mon. Notices Royal Astron. Soc.* **462**, S253–S273, DOI: 10.1093/mnras/stw2601 (2016).
7. Boice, D. C. & Reylé, C. The Nature of Diatomic Sulfur in Comets. *Highlights Astron.* **13**, 501 (2005).
8. Oppenheimer, C., Scaillet, B. & Martin, R. Sulfur degassing from volcanoes: Source conditions, surveillance, plume chemistry and earth system impacts. *Rev. Mineral. Geochem.* **73**, 363–421, DOI: 10.2138/rmg.2011.73.13 (2011).
9. Karimi, M. *et al.* Reactivity of disulfide bonds is markedly affected by structure and environment: Implications for protein modification and stability. *Sci. Reports* **6**, 38572, DOI: 10.1038/srep38572 (2016).
10. Dyke, J. M. Properties of gas-phase ions. Information to be obtained from photoelectron spectroscopy of unstable molecules. *J. Chem. Soc., Faraday Trans. 2* **83**, 69–87, DOI: 10.1039/F29878300069 (1987).
11. Molloy, R., Danielsson, A., Karlsson, L. & Eland, J. Double photoionisation spectra of small molecules and a new empirical rule for double ionisation energies. *CHEMICAL PHYSICS* **335**, 49–54 (2007).
12. Mahajan, C., Lakshminarayana, G. & Narasimham, N. Rydberg transitions of S2. *Indian J. Pure & Appl. Phys. (IJPAP)* **14**, 488–490 (1976).

**13.** Zavilopulo, A., Markush, P., Shpenik, O. & Mykyta, M. Electron-impact ionization and dissociative ionization of sulfur in the gas phase. *Tech. Phys.* **59**, 951–958, DOI: 10.1134/S1063784214070299 (2014).

**14.** Berkowitz, J. & Marquart, J. R. Equilibrium composition of sulfur vapor. *The J. Chem. Phys.* **39**, 275–283, DOI: 10.1063/1.1734241 (1963).

**15.** Eland, J. H. D. & Feifel, R. Double ionisation of ICN and BrCN studied by a new photoelectron photoion coincidence technique. *Chem. Phys.* **327**, 85–90, DOI: 10.1016/j.chemphys.2006.03.040 (2006).

**16.** Feifel, R., Eland, J. H. D., Storchi, L. & Tarantelli, F. An experimental and theoretical study of double photoionization of $CF_4$ using time-of-flight photoelectron-photoelectron (photoion-photoion) coincidence spectroscopy. *J. Chem. Phys.* **125**, 194318–194318, DOI: 10.1063/1.2386154 (2006).

**17.** Wiley, W. C. & McLaren, I. H. Time-of-flight mass spectrometer with improved resolution. *Rev. Sci. Instruments* **26**, 1150–1157, DOI: 10.1063/1.1715212 (1955). https://doi.org/10.1063/1.1715212.

**18.** Plogmaker, S. *et al.* Versatile high-repetition-rate phase-locked chopper system for fast timing experiments in the vacuum ultraviolet and x-ray spectral region. *Rev. Sci. Instruments* **83**, 013115, DOI: 10.1063/1.3677329 (2012).

**19.** Eland, J. H. D., Feifel, R. & Edvardsson, D. Single and double photoelectron spectroscopy of atomic mercury. *The J. Phys. Chem. A* **108**, 9721–9725, DOI: 10.1021/jp040332g (2004).

**20.** Knowles, P. J. & Werner, H.-J. An efficient second-order MC SCF method for long configuration expansions. *Chem. Phys. Lett.* **115**, 259–267, DOI: 10.1016/0009-2614(85)80025-7 (1985).

**21.** Werner, H.-J. & Knowles, P. J. A second order multiconfiguration SCF procedure with optimum convergence. *The J. Chem. Phys.* **82**, 5053–5063, DOI: 10.1063/1.448627 (1985).

**22.** Werner, H. & Knowles, P. J. An efficient internally contracted multiconfiguration–reference configuration interaction method. *The J. Chem. Phys.* **89**, 5803–5814, DOI: 10.1063/1.455556 (1988).

**23.** Knowles, P. J. & Werner, H.-J. An efficient method for the evaluation of coupling coefficients in configuration interaction calculations. *Chem. Phys. Lett.* **145**, 514–522, DOI: 10.1016/0009-2614(88)87412-8 (1988).

**24.** Shamasundar, K. R., Knizia, G. & Werner, H.-J. A new internally contracted multi-reference configuration interaction method. *The J. Chem. Phys.* **135**, 054101, DOI: 10.1063/1.3609809 (2011).

**25.** Werner, H.-J., Knowles, P. J., Knizia, G., Manby, F. R. & Schütz, M. Molpro: a general-purpose quantum chemistry program package. *WIREs Comput. Mol. Sci.* **2**, 242–253, DOI: https://doi.org/10.1002/wcms.82 (2012). https://wires.onlinelibrary.wiley.com/doi/pdf/10.1002/wcms.82.

**26.** Werner, H.-J. *et al.* Molpro, version 2015, a package of ab initio programs.

**27.** Kendall, R. A., Dunning, T. H. & Harrison, R. J. Electron affinities of the first-row atoms revisited. systematic basis sets and wave functions. *The J. Chem. Phys.* **96**, 6796–6806, DOI: 10.1063/1.462569 (1992).

**28.** Woon, D. E. & Dunning, T. H. Gaussian basis sets for use in correlated molecular calculations. iii. the atoms aluminum through argon. *The J. Chem. Phys.* **98**, 1358–1371, DOI: 10.1063/1.464303 (1993).

**29.** Dunning, T. H., Peterson, K. A. & Wilson, A. K. Gaussian basis sets for use in correlated molecular calculations. x. the atoms aluminum through argon revisited. *The J. Chem. Phys.* **114**, 9244–9253, DOI: 10.1063/1.1367373 (2001).

**30.** Deegan, M. J. O. & Knowles, P. J. Perturbative corrections to account for triple excitations in closed and open shell coupled cluster theories. *Chem. Phys. Lett.* **227**, 321–326, DOI: 10.1016/0009-2614(94)00815-9 (1994).

**31.** Hampel, C., Peterson, K. A. & Werner, H.-J. A comparison of the efficiency and accuracy of the quadratic configuration interaction (QCISD), coupled cluster (CCSD), and Brueckner coupled cluster (BCCD) methods. *Chem. Phys. Lett.* **190**, 1–12, DOI: 10.1016/0009-2614(92)86093-W (1992).

**32.** Knowles, P. J., Hampel, C. & Werner, H.-J. Erratum: "Coupled cluster theory for high spin, open shell reference wave functions" [ J. Chem. Phys. 99, 5219 (1993)]. *The J. Chem. Phys.* **112**, 3106–3107, DOI: 10.1063/1.480886 (2000).

**33.** Cooley, J. W. An improved eigenvalue corrector formula for solving the schrodinger equation for central fields. *Math. Comput.* **15**, 363–374 (1961).

**34.** Yee, K. K., Barrow, R. F. & Rogstad, A. Resonance fluorescence and raman spectra of gaseous sulphur. *J. Chem. Soc., Faraday Trans. 2* **68**, 1808–1811, DOI: 10.1039/F29726801808 (1972).

**35.** Freedman, P. A., Jones, W. J. & Rogstad, A. Rotational raman spectrum of sulphur dimer. *J. Chem. Soc., Faraday Trans. 2* **71**, 286–292, DOI: 10.1039/F29757100286 (1975).

**36.** Wayne, F. D., Davies, P. B. & Thrush, B. A. The gas-phase E.P.R. spectrum of diatomic sulphur molecules. *Mol. Phys.* **28**, 989–996, DOI: 10.1080/00268977400102311 (1974).

**37.** Channappa, K., Pendlebury, J. & Smith, K. Atomic beam radiofrequency spectroscopy of $S^{32}$ $S^{32}$ molecules. *La structure hyperfine magnetique des atomes et des molecules* 73–81 (1967).

**38.** Brabaharan, K. & Coxon, J. Rotational analysis of the $A^2\Pi_u \rightarrow X^2\Pi_g$ system of $^{32}S_2^+$. *J. Mol. Spectrosc.* **128**, 540–553, DOI: 110.1016/0022-2852(88)90169-5 (1988).

**39.** Sun, Z. F., Farooq, Z., Parker, D. H., Martin, P. J. J. & Western, C. M. Photodissociation of S2 ($X\,^3\Sigma_g^-$, $a\,^1\Delta_g$, and $b\,^1\Sigma_g^+$) in the 320–205 nm Region. *The J. Phys. Chem. A* **123**, 6886–6896, DOI: 10.1021/acs.jpca.9b05350 (2019). PMID: 31322887, https://doi.org/10.1021/acs.jpca.9b05350.

**40.** Huttula, M. *et al.* Spectroscopy of triply and quadruply ionized states of mercury. *Phys. Rev. A* **83**, DOI: 10.1103/PhysRevA.83.032510 (2011).

**41.** Huttula, M. & Huttula, S.-M. Core-valence double photoionization of atomic mercury. *Phys. Rev. A* **89**, DOI: 10.1103/PhysRevA.89.013411 (2014).

**42.** Hall, R. I., Dawber, G., McConkey, A., MacDonald, M. A. & King, G. C. Vibrational structure of the $O_2^{2+}$ ground state observed by threshold photoelectron coincidence spectroscopy. *Phys. Rev. Lett.* **68**, 2751–2754, DOI: 10.1103/PhysRevLett.68.2751 (1992).

**43.** Feifel, R., Eland, J. H. D. & Edvardsson, D. Valence double ionization of O2 at photon energies below and above the molecular double ionization threshold. *The J. Chem. Phys.* **122**, 144308, DOI: 10.1063/1.1872836 (2005). https://doi.org/10.1063/1.1872836.

**44.** Lias, S. G. *et al. NIST Chemistry WebBook, NIST Standard Reference Database Number 69, Eds. P.J. Linstrom and W.G. Mallard*, chap. Ion Energetics Data (National Institute of Standards and Technology, Gaithersburg MD, 20899, 2022). (retrieved May 13, 2022).

**45.** Eland, J. H. Complete double photoionisation spectra of small molecules from tof-pepeco measurements. *Chem. Phys.* **294**, 171–186, DOI: https://doi.org/10.1016/j.chemphys.2003.08.001 (2003).

**46.** Lundqvist, M., Edvardsson, D., Baltzer, P., Larsson, M. & Wannberg, B. Observation of predissociation and tunnelling processes in : a study using doppler free kinetic energy release spectroscopy and ab initio ci calculations. *J. physics. B, At. molecular, optical physics* **29**, 499 (1996).